Ammonia Decomposition in Catalytic Membrane Reactors: Simulation and Experimental Studies

Gang Li, Masakoto Kanezashi, Tomohisa Yoshioka, and Toshinori Tsuru
Dept. of Chemical Engineering, Hiroshima University, Higashi-Hiroshima 739-8527, Japan

DOI 10.1002/aic.13794
Published online April 16, 2012 in Wiley Online Library (wileyonlinelibrary.com).

Catalytic decomposition of NH_3 with H_2-selective microporous silica membranes for CO_x-free hydrogen production was studied theoretically and experimentally. The simulation study shows that NH_3 conversion, H_2 yield and H_2 purity increase with the Damköhler number (Da), and their improvement is affected by the effect of H_2 extraction as well as NH_3 and N_2 permeation through the membranes. The experimental study of NH_3 decomposition was carried out in a bimodal catalytic membrane reactor (BCMR), consisting of a bimodal catalytic support and a H_2-selective silica layer. Catalytic membranes showed H_2 permeances of 6.2–9.8 $\times$ 10^{-7} mol m^{-2} s^{-1} Pa^{-1}, with H_2/NH_3 and H_2/N_2 permeance ratios of 110–200 and 200–700, respectively, at 773 K. The effect of operating conditions on membrane reactor performance with respect to NH_3 conversion, H_2 yield and H_2 purity was investigated, and the results were in agreement with those calculated by the proposed simulation model. © 2012 American Institute of Chemical Engineers *AIChE J,* 59: 168–179, 2013
Keywords: ammonia decomposition, catalytic membrane reactor, silica membrane, CO_x-free hydrogen, hydrogen production

Introduction

A major obstacle to the use of hydrogen as a widespread energy carrier is its storage, due to the low-volumetric density of gaseous hydrogen. Liquid hydrogen can have a high-volumetric density of 70 kg m^{-3}; its liquefaction, however, requires an extremely low temperature, below 23 K, with a loss of about 30% of the chemical energy of gaseous hydrogen.[1] This cryogenic process is, thus, not feasible for practical application. Ammonia, which is well-known as a raw material for the nitrogenous fertilizer industry and has been commercialized on a large scale using the Haber process, was recently proposed as an ideal hydrogen carrier for the purpose of hydrogen storage and delivery because of its unique characteristics.[2–4] NH_3 has a high-hydrogen storage capacity (17.6 wt %), and can be readily stored as a liquid under ambient temperature when a mild pressure of $\sim$ 0.8 MPa is applied, producing a very high-hydrogen volumetric density of 120 kg m^{-3},[5] which is much higher than that of liquid hydrogen. Importantly, NH_3 is carbon free at the point of use, it produces CO_x-free hydrogen after decomposition requiring neither further processing to capture the CO_2 that is mainly responsible for the greenhouse effect, nor selective oxidation of CO that can poison the electrodes of proton exchange fuel cells even at an extremely low concentration. In addition, the infrastructure for NH_3 storage and delivery has already been well-established world-wide, so massive investments and technical efforts in the development of a new system for hydrogen can be avoided. These great advantages make the use of NH_3 as a medium for hydrogen storage and delivery extremely attractive. As a result of the potential implementation of a NH_3-mediated H_2 economy, NH_3 decomposition for CO_x-free H_2 production has, therefore, attracted tremendous attention in recent years.[6–13]

On the other hand, substantial progress in the area of membrane science and technology has greatly promoted an increasing interest in membrane reaction. Various types of membrane reactors, such as Pd and Pd alloys,[14–16] zeolite,[17,18] silica,[7,19–21] etc., have been widely used in catalytic reactions for enhanced catalytic performance. The application of membrane reactors appears to be a very promising route for the production of H_2 from NH_3 decomposition, since the improved NH_3 conversion and purified H_2 can be obtained simultaneously after H_2 extraction using a H_2-selective membrane. However, only a few studies of NH_3 decomposition in membrane reactors have been reported, and costly Pd membranes were typically adopted since they are only permeable for H_2. Collins and Way[16] reported the catalytic decomposition of NH_3 in a packed-bed Pd membrane reactor, in an attempt to reduce the trace amount of NH_3 produced in the process of coal gasification, showing enhanced NH_3 conversion compared with a conventional reactor. A study by García-García et al.[9] investigated diluted NH_3 decomposition in a packed-bed Pd membrane reactor for CO_x-free hydrogen production, and NH_3 conversion that exceeded the thermodynamic equilibrium limit was obtained after H_2 extraction. Zhang et al.[10] applied a packed-bed Pd membrane reactor to pure NH_3 decomposition for the generation of CO_x-free hydrogen, and found that the removal of H_2 product from the reactor significantly improved the NH_3 conversion. Although Pd membranes show an extremely

Correspondence concerning this article should be addressed to T. Tsuru at tsuru@hiroshima-u.ac.jp.

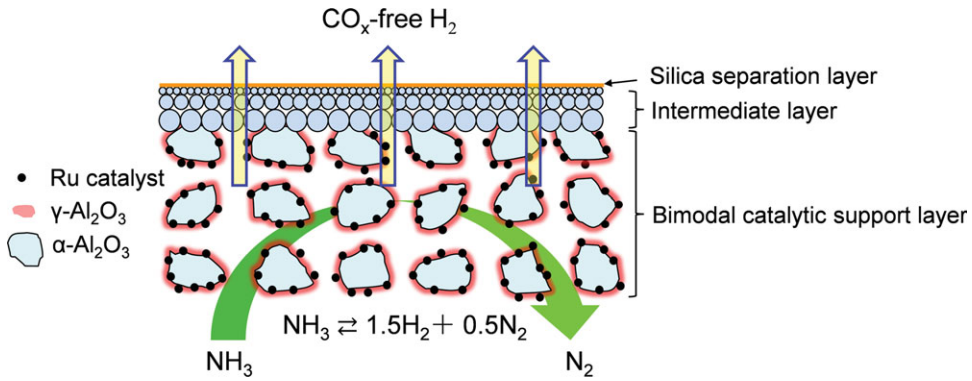

Figure 1. Schematic diagram of the bimodal catalytic membrane reactor.

[Color figure can be viewed in the online issue, which is available at wileyonlinelibrary.com.]

high selectivity for hydrogen separation, taking the cost into account, challenges still remain for their practical application on a large scale.

We recently proposed a novel bimodal catalytic membrane reactor (BCMR) for NH_3 decomposition.[7] As shown in Figure 1, the BCMR consisted of a bimodal catalytic layer and a H_2-selective silica layer. The bimodal structure was formed by impregnation of γ-Al_2O_3 with mesopores into macroporous α-Al_2O_3 membrane supports, which was expected to enhance the catalytic performance due to improved catalyst dispersion by mesopores and fast-gas diffusion by macropores.[7,20,21] Moreover, silica membranes, compared with Pd membranes, could greatly reduce the cost of membrane reactor preparation. NH_3 conversion was highly enhanced from 45 to 95% in the membrane reactor after H_2 extraction at 723 K, and the BCMR showed excellent stability with respect to catalytic activity and separation performance in a NH_3 atmosphere.[7] However, additional theoretical and experimental investigation is yet required in order to clarify the details of the effects of various parameters, such as membrane characteristics and operating conditions, on membrane reactor performance.

In this study, NH_3 decomposition in a BCMR was proposed for CO_x-free hydrogen production. A mathematical model was formulated for the simulation study of NH_3 decomposition in a cocurrent configuration membrane reactor, and the effect of Damköhler number (Da), permeation number (θ), and membrane selectivity on membrane reactor performance was discussed theoretically. In addition, an experimental study was conducted to investigate the effects of operating conditions (e.g., reaction temperature, NH_3 feed flow rate and sweep flow rate) on membrane reactor performance in terms of NH_3 conversion, H_2 yield and H_2 purity, and the results were compared with those predicted by the proposed simulation model.

Simulation

The simulation study of NH_3 decomposition in catalytic membrane reactors was performed based on the following assumptions (1) steady-state operation, (2) plug flow in both feed and permeate streams, (3) an isothermal reaction, which only occurs over the catalyst on the feed side, (4) negligible pressure drop along the axial direction of the membrane reactor, and (5) no concentration polarization effect for gas permeation through the membrane. A schematic model for membrane reactor simulation is shown in Figure 2.

For a plug-flow type membrane reactor, the molar flow rate for each component in the feed and permeate streams can be expressed as follows[19,22]:

Feed stream

$$\frac{dF_i}{dz} = v_i R w_{cat} - sP_i(x_i p_h - y_i p_l) \tag{1}$$

Permeate stream

$$\frac{dQ_i}{dz} = sP_i(x_i p_h - y_i p_l) \tag{2}$$

where F_i and Q_i are the flow rates of the i-th component in the feed and permeate streams, and the corresponding mole fractions are indicated as x_i and y_i, respectively. z indicates the axial direction along the membrane, P_i is the permeance of the i-th component through the membrane, v_i is the stoichiometric coefficient of the i-th component, w_{cat} and s represent the catalyst weight and membrane area per membrane unit length, and, p_h and p_l indicate the total pressure of the feed and permeate streams, respectively. R is defined as the reaction rate of NH_3 decomposition, which can be expressed by the Temkin-Pyzhev model[23] based on the following reaction equation

$$NH_3 \rightleftharpoons 0.5N_2 + 1.5H_2 \tag{3}$$

$$R = k\left[\left(\frac{p_{NH_3}^2}{p_{H_2}^3}\right)^{\beta} - \frac{p_{N_2}}{K_{eq}^2}\left(\frac{p_{H_2}^3}{p_{NH_3}^2}\right)^{(1-\beta)}\right] \tag{4}$$

where

$$k = k_0 \exp\left(\frac{-E_a}{R_g T}\right) \tag{5}$$

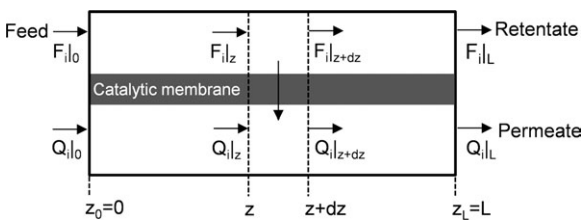

Figure 2. Schematic model for membrane reactor simulation.

Table 1. Dimensionless Numbers Used in the Simulation

Dimensionless number	Symbol	Definition
Damköhler number	Da	$Da = R^{\max} W_{cat} / F_{NH_3,0}$
Permeation number	θ	$\theta = P_{H_2} s L p_h / F_{NH_3,0}$
Reaction rate ratio	R^*	$R^* = R/R^{\max}$
Pressure ratio	p_r	$p_r = p_l/p_h$
Permeance ratio	$\alpha_{H_2/i}$	$\alpha_{H_2/i} = P_{H_2}/P_i$
Axial position	ζ	$\zeta = z/L$

and

$$K_{eq} = \frac{p_{H_2,eq}^{1.5} p_{N_2,eq}^{0.5}}{p_{NH_3,eq}} \tag{6}$$

k is the reaction rate constant; K_{eq} is the equilibrium constant for the NH_3 decomposition reaction based on the equilibrium partial pressure of each component, and can be calculated by thermodynamic analysis. k_0 and E_a indicate the pre-exponential factor and activation energy of the catalyst for NH_3 decomposition, respectively. β is the exponential constant related to reaction order depending on the catalyst used. For an alumina-supported Ru catalyst, Prasad et al.[12] obtained $\beta = 0.27$, $E_a = 117$ kJ mol^{-1}, and $k_0 = 6.0 \times 10^8$ s^{-1} (turnover frequency) under atmospheric pressure, which were used for the calculations in this simulation study.

With the aid of dimensionless numbers, as listed in Table 1, Eqs. 1 and 2 can be further expressed as dimensionless equations:

Feed stream

$$\frac{df_i}{d\zeta} = v_i R^* Da - \frac{\theta(x_i - y_i p_r)}{\alpha_{H_2/i}} \tag{7}$$

Permeate stream

$$\frac{dq_i}{d\zeta} = \frac{\theta(x_i - y_i p_r)}{\alpha_{H_2/i}} \tag{8}$$

where f_i and q_i are the dimensionless flow rates of the i-th component normalized by the NH_3 feed flow rate in the feed and permeate streams, respectively. R^* and p_r are the dimensionless reaction rate and pressure, which correspond to the ratio of reaction rate R to the maximum reaction rate $R^{\max}$ based on the inlet feed composition, and the pressure ratio of permeate stream to feed stream, respectively. The Damköhler number, Da, is defined as the ratio of the arithmetic product of the maximum reaction rate $R^{\max}$ and catalyst weight of membrane module W_{cat} to the inlet NH_3 feed flow rate, which can serve as a measure of space velocity in the membrane reactor. A high Damköhler number can be obtained when either a high-catalyst loading or low NH_3 feed flow rate is adopted, and the higher the Damköhler number, the closer the reaction is to equilibrium conversion. The permeation number, θ, is defined as the ratio of the maximum H_2 permeation flow rate to the inlet NH_3 feed flow rate, which can act as a measure of the H_2 extraction effect. A higher permeation number indicates that more H_2 can be removed from the membrane reactor. Since membrane reactor performance is determined by the overall effect of catalytic activity, membrane performance, and operating conditions, the use of the two independent dimensionless numbers, Da and θ, makes quantitative insight into the influence of each parameter on membrane reactor performance much easier and more convenient.

The simulation of pure NH_3 decomposition was conducted in concurrent configuration membrane reactors at 723 K, with silica membranes showing H_2/NH_3 selectivities over a wide range (10-∞), under feed and permeate pressures of 100 kPa and 5 kPa, respectively. The large molecules, NH_3 and N_2, were assumed to mainly permeate through the large pores in the silica membranes, showing Knudsen selectivity for the gas pair of NH_3-N_2 based on a Knudsen diffusion mechanism. The Damköhler number, permeation number, and membrane selectivity were adopted as parameters to study their effect on membrane reactor performance in terms of NH_3 conversion, H_2 yield and H_2 purity. It should be noted that the initial reaction rate would be infinite according to the Temkin-Pyzhev model when the feed is pure NH_3, since the H_2 partial pressure is in the denominator. To solve this kind of problem, it has been suggested that a small amount of H_2 was added in the feed for simulation studies of methane steam reforming.[19,24,25] In this study, the same technique was used and the partial pressure ratio of H_2 to NH_3 in the feed was set in the range of 10^{-2} –10^{-3} as the initial conditions for simulation, which showed almost the same NH_3 conversion.

Experimental

Preparation and characterization of silica membranes

Porous α-Al_2O_3 tubes (porosity: $\sim$ 50%; average pore size: 1 μm; outer diameter: 10 mm; inner diameter: 8 mm; length: 10 cm) were used as supports for membrane preparation. Briefly, each support was first sealed with glass tubes at both ends, and then one of the ends was sealed as a dead-end. A boehmite sol solution (10 wt % Nissan Chemical Industries, Ltd., Japan) was impregnated into the support. After drying at room temperature, the support was calcined at 823 K for 1 h to convert the sols impregnated in the macropores of the support into γ-Al_2O_3, resulting in a γ-Al_2O_3/α-Al_2O_3 bimodal support. Then, the support was soaked in a $Ru(NO)(NO_3)_3$ solution (1.5 wt % based on Ru, Sigma-Aldrich) followed by drying at room temperature overnight and calcination at 823 K for 1 h to bimodal catalytic support. After the preparation of an α-Al_2O_3 particle and SiO_2-ZrO_2 intermediate layer on the outer surface of the obtain bimodal catalytic support, polyhedral oligometric silsequioxane (POSS)-derived silica sols were coated on the support, subsequently dried at 573 K, and calcined at 773 K for 30 min to form a homogeneous (HOMO)-POSS-derived silica membrane. Details of the preparation of HOMO-POSS-derived silica sols and membranes were shown in a previous study.[26]

Gas permeation tests of single components of He, H_2, NH_3 and N_2 were used to evaluate the HOMO-POSS-derived silica membranes. The measurements were conducted at 473–773 K, under the feed and permeate pressures of 200 and 100 kPa, respectively. Prior to the measurement, all the membranes were kept in a He flow of 3.72×10^{-5} mol s^{-1} at 473 K to remove the adsorbed water from the membranes. The gas flow rate from the permeation cell was measured directly by a bubble flow meter, with the exception of the measurement of NH_3. For the NH_3 permeation test, 7.44×10^{-6} mol s^{-1} sweep gas was applied to the permeate side, and the gas composition of the permeate stream was analyzed by a gas chromatograph (GC) instrument (GC-14B, Shimadzu) equipped with a thermal conductivity detector (TCD) and a Porapak N column using N_2 as a carrier gas. The membrane morphology and thickness were examined by scanning electron microscopy (SEM) (JCM-5700, JEOL). A schematic

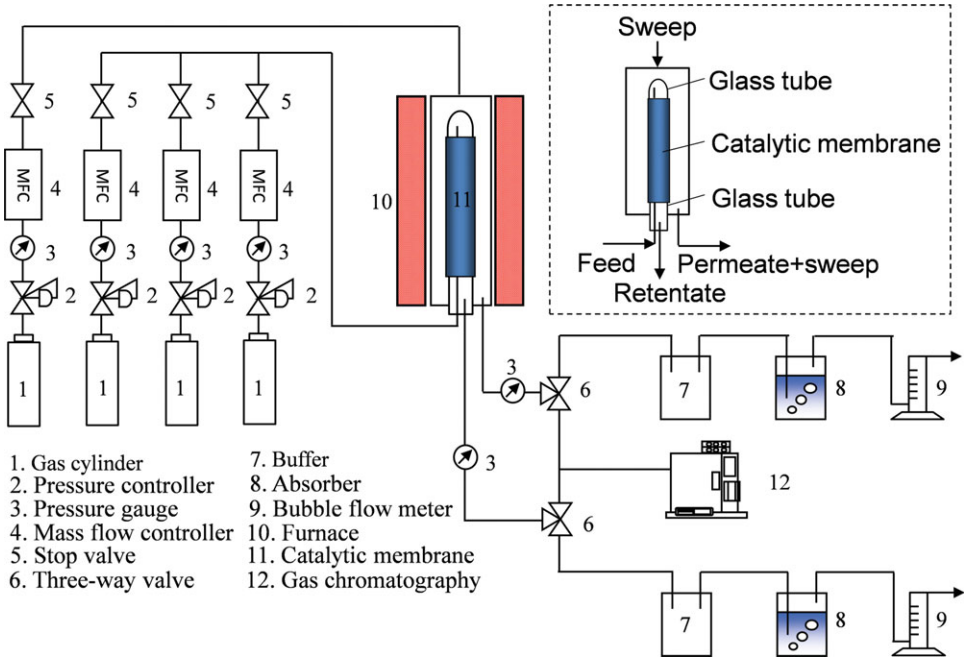

Figure 3. Experimental apparatus for single gas permeation tests and NH_3 decomposition.

[Color figure can be viewed in the online issue, which is available at wileyonlinelibrary.com.]

diagram of the experimental apparatus for single gas permeation tests and NH_3 decomposition is shown in Figure 3.

NH_3 decomposition in catalytic membrane reactors

Pure NH_3 decomposition was performed in BCMRs at 663–743 K, with both feed and permeate streams kept at atmospheric pressure. Prior to the membrane reaction, the catalytic membranes were reduced *in situ* in the membrane reactor under a H_2 flow of 3.72×10^{-5} mol s^{-1} at 773 K for 3 h, and then 3.72×10^{-5} mol s^{-1} N_2 flow was introduced to flush the experimental apparatus for 30 min. Feed NH_3 was introduced to the dead-end zone of catalytic membranes through a stainless steel tube inside the membrane tubes with a flow rate that ranged from 7.44×10^{-6}–3.72×10^{-5} mol s^{-1}. N_2 sweep gas was applied to the shell side of the membrane reactors in order to remove H_2 from the permeate stream to maintain the H_2 partial pressure difference between retentate and permeate sides, resulting in a driving force for H_2 permeation through the membranes. The gas composition of both retentate and permeate streams was analyzed by GC, and the flow rate was measured after leading the gases through a 1.0 M HCl aqueous solution. NH_3 conversion (X), H_2 yield (Y), and H_2 purity (G) (excluding sweep gas), obtained in the membrane reactor after H_2 extraction with sweep, were defined as follows

$$X = \frac{F_{NH_3,0} - F_{NH_3,L} - Q_{NH_3,L}}{F_{NH_3,0}} \tag{9}$$

$$Y = \frac{2Q_{H_2,L}}{3F_{NH_3,0}} \tag{10}$$

$$G = \frac{Q_{H_2,L}}{Q_{NH_3,L} + Q_{N_2,L} + Q_{H_2,L}} \tag{11}$$

The following definitions were used when no sweep was applied to the membrane reactor

$$X = \frac{F_{NH_3,0} - F_{NH_3,L}}{F_{NH_3,0}} \tag{12}$$

$$Y = \frac{2F_{H_2,L}}{3F_{NH_3,0}} \tag{13}$$

$$G = \frac{F_{H_2,L}}{F_{NH_3,L} + F_{N_2,L} + F_{H_2,L}} \tag{14}$$

Results and Discussion

Simulation study of membrane reactors

Figure 4 shows the axial profiles of H_2 partial pressure normalized by feed pressure, and each component flow rate normalized by feed NH_3 in the membrane reactor at 723 K under both a Damköhler number, Da, and a permeation number, θ, of 30 with a H_2/NH_3 permeance ratio of 200. In retentate stream, the normalized flow rate of NH_3 gradually decreases along the axis while it increases for N_2, because the catalytic decomposition of NH_3 occurs over the catalysts. The normalized flow rate of H_2 initially increases and then decreases along the axis due to the change in the rates of both H_2 generation and permeation along the axial direction, and it is much lower than that of N_2 at the outlet of the reactor. On the other hand, in permeate stream, the normalized H_2 flow rate greatly increases to 1.38 at the outlet of the membrane reactor, which was much higher than that of retentate side. The normalized N_2 and NH_3 flow rates are very small at any axial position. This is because the membrane is highly permeable for H_2 over N_2 and NH_3, and thus most of the H_2 produced can easily permeate through the membrane from the reaction side to permeate side due to the H_2 partial difference across the membrane, but permeation is greatly retarded for N_2 and NH_3. Although the presence of NH_3 is observed in permeate stream, the concentration of NH_3 can be easily reduced to less than 200 ppb by leading the gas mixture through a suitable adsorber.[6,11]

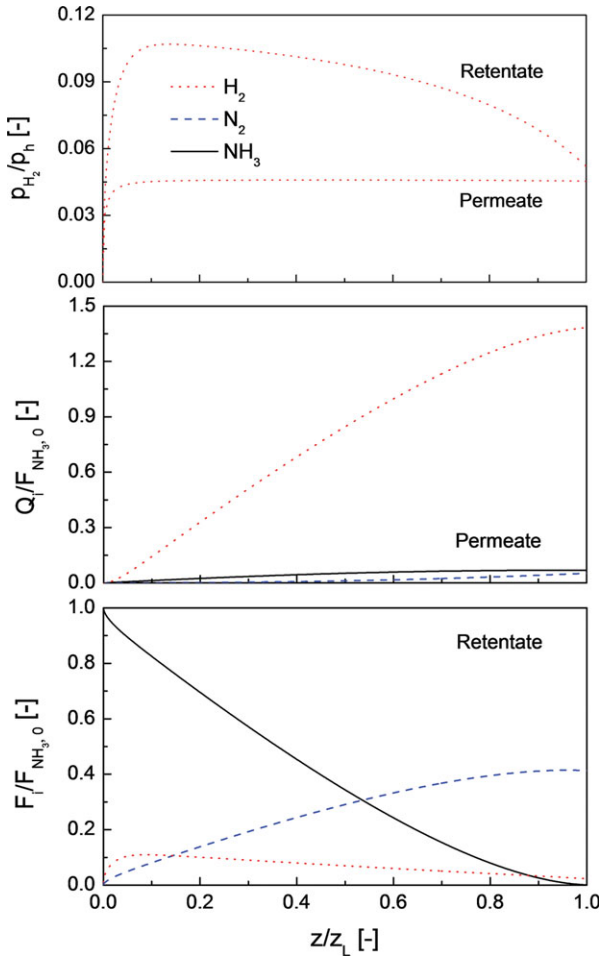

Figure 4. Axial profiles of H_2 partial pressure normalized by feed pressure and each component flow rate normalized by NH_3 feed in the membrane reactor (T = 723 K; p_h = 100 kPa, p_l = 5 kPa; α_{H_2/NH_3} = 200, α_{NH_3/N_2} = Knudsen selectivity; Da = 30; θ = 30).

[Color figure can be viewed in the online issue, which is available at wileyonlinelibrary.com.]

Figure 5 shows the effect of Damköhler number on NH_3 conversion, H_2 yield, and H_2 purity as a function of permeation number. NH_3 conversion increases with increasing Da, due to the decreased space velocity, which can be achieved by using a large catalyst loading or a small NH_3 feed flow rate. When the Da is 5, NH_3 conversion gradually increases as the θ increases from 0.1 to 100. At Da values of 30 and 100, NH_3 conversion initially increases and then decreases with increasing θ. When the Da is increased to 300, NH_3 conversion increases to approximately 100% regardless of θ. These differences in the dependence of NH_3 conversion on the permeation number can mainly be ascribed to the total effect of H_2 extraction and NH_3 reactant loss on membrane reactor performance, since the silica membrane is permeable for both H_2 and NH_3 molecules. Generally, the selective H_2 extraction contributes to the improvement of NH_3 conversion due to the increased reaction rate.[7] On the other hand; the loss of NH_3 reactant adversely affects NH_3 conversion because less reactant participates in the decomposition reaction, which only occurs on the catalysts on the feed side of the membrane reactor. At a low Da of 5, which corresponds to a low-catalytic activity, H_2 extraction improves catalytic performance as the θ increased due to the increased H_2 extraction. On the other hand, at a high Da of 300, NH_3 conversion proceeds at an extremely high reaction rate, resulting in NH_3 conversion that almost approaches equilibrium conversion, that is, almost 100% at 723 K and the effects of H_2 extraction and NH_3 loss were not important. Therefore, NH_3 conversion is almost 100%, regardless of θ. The maximum NH_3 conversion for Da values of 30 and 100 can be mainly attributed to balance of the effect of H_2 extraction and NH_3 loss as θ increases.

The H_2 yield, defined as Eq.10, is determined by both the amount of H_2 produced from NH_3 decomposition and the H_2 extraction from the reaction side in the membrane reactor. As shown in Figure 5, H_2 yield increases with an increase in Da, which can be ascribed to improved NH_3 conversion. For a given Da of 5, the H_2 yield increases gradually with increasing θ since more H_2 can permeate from the reaction side to permeate side. However, a maximum H_2 yield is observed for the Da values of 30 and 100, for the same reason as for the maximum NH_3 conversion previously explained. The H_2 purity obtained in permeate stream decreases as the θ increases from 0.1 to 100 for any value of

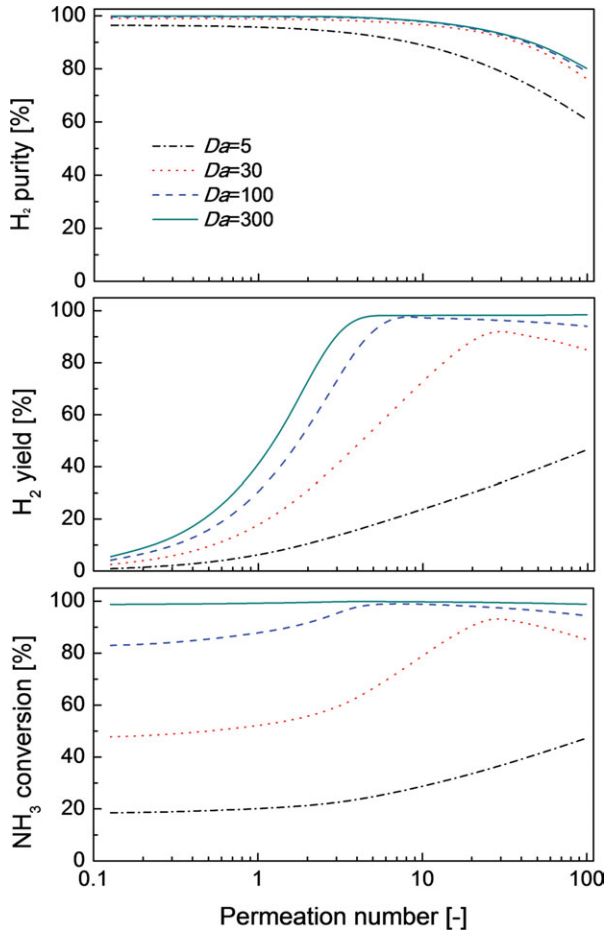

Figure 5. Effect of Damköhler number on NH_3 conversion, H_2 yield, and H_2 purity as a function of permeation number (T = 723 K; p_h = 100 kPa, p_l = 5 kPa; α_{H_2/NH_3} = 200, α_{NH_3/N_2} = Knudsen selectivity).

[Color figure can be viewed in the online issue, which is available at wileyonlinelibrary.com.]

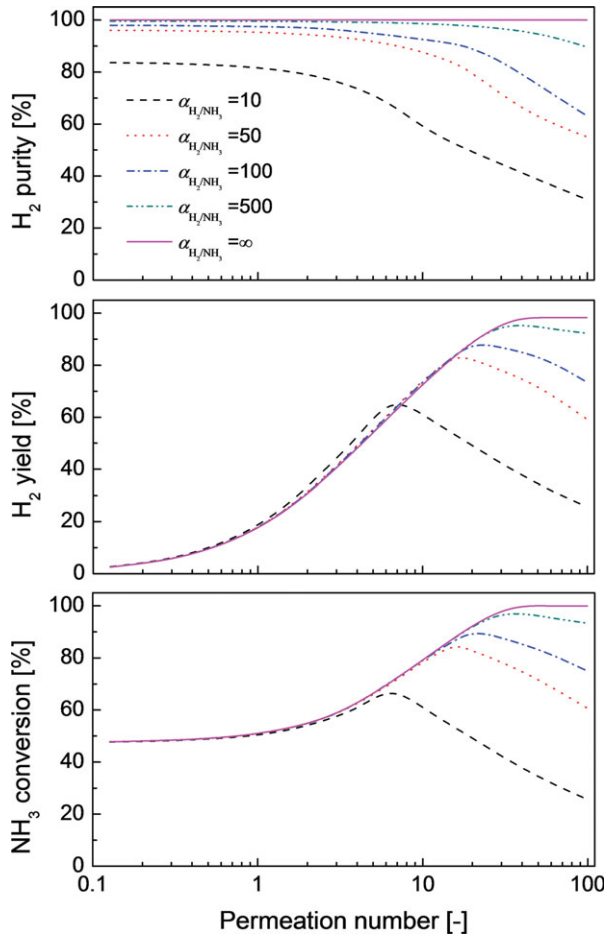

Figure 6. Effect of H_2/NH_3 selectivity on NH_3 conversion, H_2 yield, and H_2 purity as a function of permeation number (T = 723 K; p_h = 100 kPa, p_l = 5 kPa; Da = 30; α_{NH_3/N_2} = Knudsen selectivity).

[Color figure can be viewed in the online issue, which is available at wileyonlinelibrary.com.]

Da. Since an increase in θ causes a larger amount of H_2 permeation from the reaction side to permeate side, which greatly increases the partial pressure of NH_3 and N_2 on the reaction side, the increased driving force for NH_3 and N_2 permeation through the membrane leads to a decrease in H_2 purity as the θ increases. Moreover, the H_2 purity increases as *Da* increases for any given θ, because enhanced NH_3 decomposition on the reaction side increases H_2 partial pressure. It should be noted that the dependence of H_2 purity on the permeation number is almost the same when the value of *Da* is more than 30, due to enough H_2 production rate. These results reveal that an increase in *Da* is not an efficient route to substantial improvement in H_2 purity in the membrane reactor.

Figure 6 shows the effect of H_2/NH_3 selectivity on NH_3 conversion, H_2 yield, and H_2 purity as a function of the permeation number. For comparison with porous silica membranes, the infinite H_2/NH_3 selectivity, which corresponds to a Pd membrane, is included in this figure. For porous silica membranes with H_2/NH_3 selectivities ranging from 10 to 500 under a *Da* of 30, the maximum NH_3 conversion is observed with increasing θ due to the total effect of H_2 extraction and NH_3 reactant loss. A highly selective membrane gives a high maximum NH_3 conversion, since the loss of NH_3 reactant is less under the same reaction conditions. For the Pd membrane, NH_3 conversion increases with θ, and then almost reaches a constant level under high values of θ. A decrease in NH_3 conversion is not observed, since there is no NH_3 permeation through the Pd membrane regardless of θ. It should be noted that all porous silica membranes show almost the same dependence of NH_3 conversion on the permeation number as the Pd membrane before reaching the maximum NH_3 conversion, regardless of silica membrane selectivity. This is because the amount of lost NH_3 reactant is not large enough to effectively affect NH_3 conversion, and the H_2 extraction effect, thus, controls the reaction performance. The H_2 yield shows very similar tendencies as a function of permeation number, since H_2 obtained in the permeate stream mainly depends on the NH_3 conversion under the same θ. Interestingly, although NH_3 conversion obtained in silica membrane reactors is slightly lower that of the Pd membrane reactor before reaching the maximum NH_3 conversion, the corresponding H_2 yield obtained in silica membrane reactors is slightly higher than that of the Pd membrane reactor. This phenomenon is much more obvious for the membrane with the lowest selectivity. This can be ascribed to the increased H_2 partial pressure difference caused by NH_3 and N_2 permeation for silica membranes, resulting in an increased H_2 flux compared with that for the Pd membrane.

As reflected in the aforementioned discussion, the improvement of Pd membrane reactor performance under a given *Da* is decided only by the H_2 extraction effect; the higher the permeation number, the better the membrane reactor performance, since no other gas can permeate through the dense Pd membrane. However, for a porous silica membrane that allows N_2 and NH_3 permeation along with H_2, the effects on membrane reactor performance of H_2 extraction and N_2 and NH_3 permeation should be considered simultaneously, which makes the system much more complicated than the Pd membrane reactor. Therefore, the simulation study is very important in order to predict the required membrane performance and optimize reaction conditions for a target membrane reaction, such as NH_3 conversion, H_2 yield and H_2 purity. For autothermal decomposition of NH_3 in a membrane reactor, the operation can be achieved by combustion of the residual NH_3 and H_2 from retentate stream after it is flowed out from the membrane reactor to provide the required heat for NH_3 decomposition. Complete oxidation of 1 mol NH_3 can generate enough heat for decomposition of 5.7 mol NH_3,[27] which means that a maximum H_2 yield of 85% can be obtained in the permeate stream via the autothermal operation. To achieve autothermal decomposition of NH_3 with a target H_2 yield of 85%, the simulation analysis shows that a silica membrane with a H_2/NH_3 selectivity of 100 is theoretically high enough in an appropriate range of θ under the simulation conditions, as shown in Figure 6.

Gas permeation properties of catalytic membranes

Figure 7 shows an SEM image of a bimodal catalytic membrane. The membrane consisted of 3 typical layers: a bimodal catalytic layer, an α-Al_2O_3 particle and SiO_2-ZrO_2 intermediate layer, and a SiO_2 separation layer. The continuous, uniform SiO_2 top layer for H_2 separation had a thickness of less than 300 nm. The bimodal catalytic structure of the membrane reactor effectively improved the catalytic

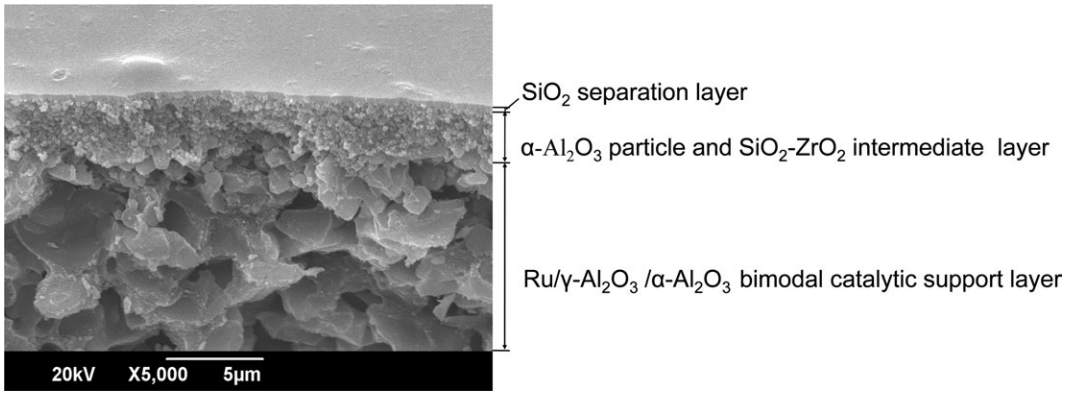

Figure 7. SEM image of a bimodal catalytic membrane.

activity and stability for supported metallic catalysts, due to improved catalyst dispersion by impregnating γ-Al_2O_3 with mesopores.[7,20,21] A decrease in membrane separation performance caused by the concentration polarization effect has been widely reported in various membrane processes.[28–32] It should be noted that the catalytic membrane configuration, in addition to being compact, allows a shorter diffusion length from catalyst to membrane surface compared with the packed-bed membrane reactor, and, thus, is expected to reduce the concentration polarization effect during the membrane reaction,[28] resulting in efficient H_2 extraction.

Figure 8 shows the gas permeance of silica membranes as a function of molecular diameter at 773 K. The BCMR-1 showed a H_2 permeance of 6.2×10^{-7} mol m^{-2} s^{-1} Pa^{-1}, with H_2/CO_2 and H_2/N_2 permeance ratios of 510 and 720, respectively, while the BCMR-2 had a looser amorphous silica structure than the BCMR-1, with a higher H_2 permeance of 9.8×10^{-7} mol m^{-2} s^{-1} Pa^{-1} and lower H_2/CO_2 and H_2/N_2 permeance ratios of 160 and 200, respectively. The high H_2/CO_2 and H_2/N_2 permeance ratios indicated that both membranes had small average pore sizes, which should be larger than the molecular size of H_2, but much less than that of CO_2 and N_2, due to the molecular sieving effect. In a previous report the kinetic diameters of NH_3, H_2, CO_2, and N_2 were determined using the Stockmayer potential as follows: He (0.26 nm), NH_3 (0.26 nm), H_2 (0.289 nm), N_2 (0.36 nm).[33] However, based on the Stockmayer potential, Leeuwen reported the molecular size of NH_3 to be 0.326 nm,[34] which was quite close to the kinetic diameter of CO_2 (0.33 nm). Previously, our group reported NH_3 permeation characteristics through amorphous silica membranes at temperatures of 323–673 K, and found that the order of gas permeance at high temperatures was as follows: He > H_2 > NH_3 > N_2.[35] A similar trend in gas permeance was also observed in this study, and the H_2/NH_3 permeance ratios for BCMR-1 and BCMR-2 were 200 and 110, respectively. Since the adsorption effect of NH_3 on silica could be negligible at high temperatures,[35] the difference in the gas permeances of each component through a silica membrane with small average pore size should be due to the difference in their molecular sizes, that is, the larger the molecular size, the lower the gas permeance. Therefore, the high H_2/NH_3 permeance ratios suggest that the actual kinetic diameter of NH_3 was much larger than that of H_2, and it is more likely that 0.326 nm is the molecular size of NH_3 for a reasonable explanation of NH_3 permeation behaviors through silica membranes.[35] These results confirmed the selective extraction of H_2 from H_2-NH_3-N_2 gas mixtures in principle based on the molecular sieving effect, which is crucial for construction of silica membrane reactors for NH_3 decomposition.

Figure 9 shows the temperature dependence of gas permeance for the BCMR-1 and the BCMR-2 in the temperature range of 473–773 K. The permeance of He and H_2 through both silica membranes increased with increasing temperature. However, the permeance of N_2 through both silica membranes appeared to be independent of temperature. Gas permeation behaviors through porous silica membranes have been known to be strongly dependent on the average pore size and on the pore size distribution of the amorphous networks.[26,35,36] Generally, when the average pore size of a silica membrane is close to the molecular sizes of He and H_2, the He and H_2 permeance increases with increasing temperature, which corresponds to the activated diffusion mechanism. However, when the average pore size of a silica membrane is much larger than the sizes of He and H_2 molecules, the He and H_2 permeance decreases with increasing temperature, which corresponds to the Knudsen diffusion

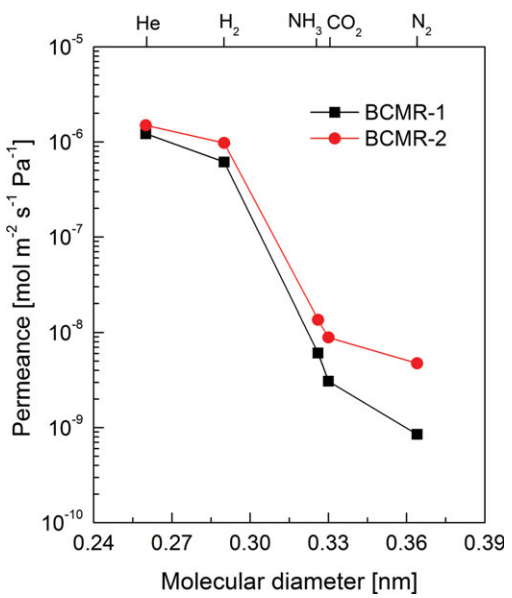

Figure 8. Molecular diameter dependence of gas permeance for the BCMR-1 and the BCMR-2 at 773 K.

[Color figure can be viewed in the online issue, which is available at wileyonlinelibrary.com.]

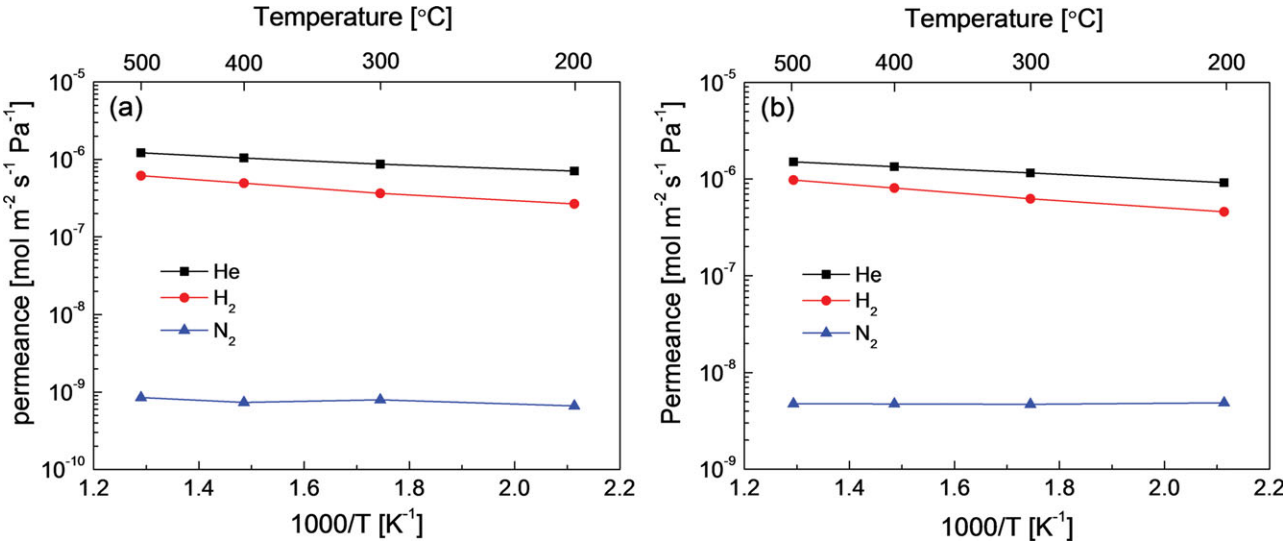

Figure 9. Temperature dependence of gas permeance for (a) the BCMR-1, and (b) the BCMR-2.

[Color figure can be viewed in the online issue, which is available at wileyonlinelibrary.com.]

mechanism. Therefore, based on the temperature dependences, the He and H_2 permeation in this study seems to be mainly dominated by the activated diffusion mechanism, indicating that both the BCMR-1 and the BCMR-2 have small pores that are close to the sizes of He and H_2 molecules. The N_2 permeation behavior appears to show the Knudsen diffusion mechanism, since N_2 is only assumed to permeate through the large pores of a membrane, such as pinholes. The average pore size of a microporous membrane relative to the H_2 molecular size can be reflected by the activation energy of the H_2 permeation through the membrane; the larger the activation energy, the smaller the average pore size. The calculated activation energies for H_2 permeation through the BCMR-1 and BCMR-2 were as high as 11.4 and 10.4 kJ mol^{-1}, respectively. These values were within the reported range for silica H_2 separation membranes, depending on preparation methods and conditions (~8–20 kJ mol^{-1}),[26,35,37–39] further confirming that the silica networks had a small average pore size, which was necessary for H_2 separation.

Time course of NH_3 decomposition in membrane reactors

Figure 10 shows the time course of NH_3 decomposition up to 120 h using BCMR-1 at 723 K with a NH_3 feed flow

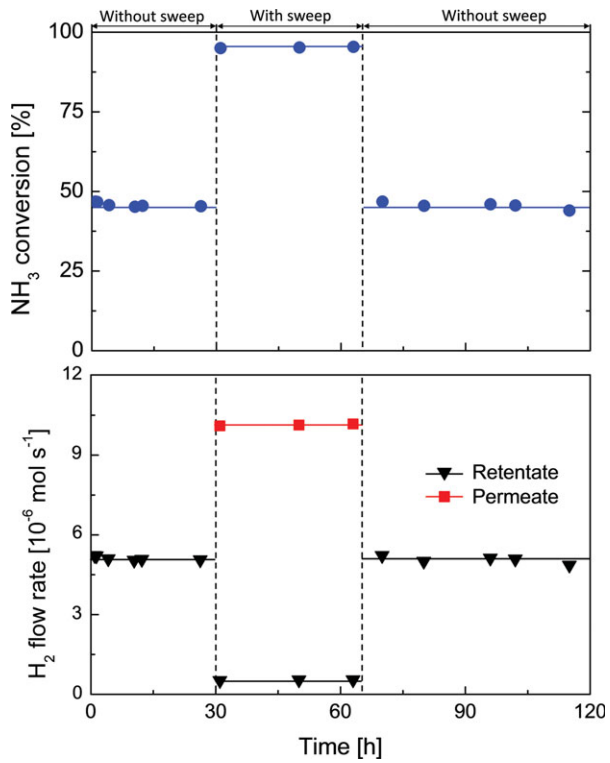

Figure 10. Time course of NH_3 decomposition in the BCMR-1 with and without sweep (T = 723 K; p_h = 100 kPa, p_l = 100kPa; $F_{NH_3,0}$ = 7.44 × 10^{-6} mol s^{-1}; $Q_{sweep,0}$ = 7.44 × 10^{-5} mol s^{-1}; α_{H_2/NH_3} = 180, α_{H_2/N_2} = 700).

[Color figure can be viewed in the online issue, which is available at wileyonlinelibrary.com.]

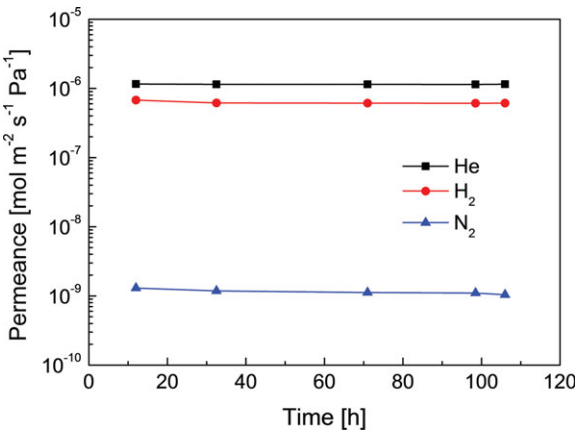

Figure 11. Stability of gas permeation properties of the BCMR-1 during the membrane reaction (T = 773 K; p_h = 200 kPa, p_l = 100 kPa; 0–30 h and 65–120 h: without sweep for NH_3 decomposition, 30–65 h: with sweep for NH_3 decomposition).

[Color figure can be viewed in the online issue, which is available at wileyonlinelibrary.com.]

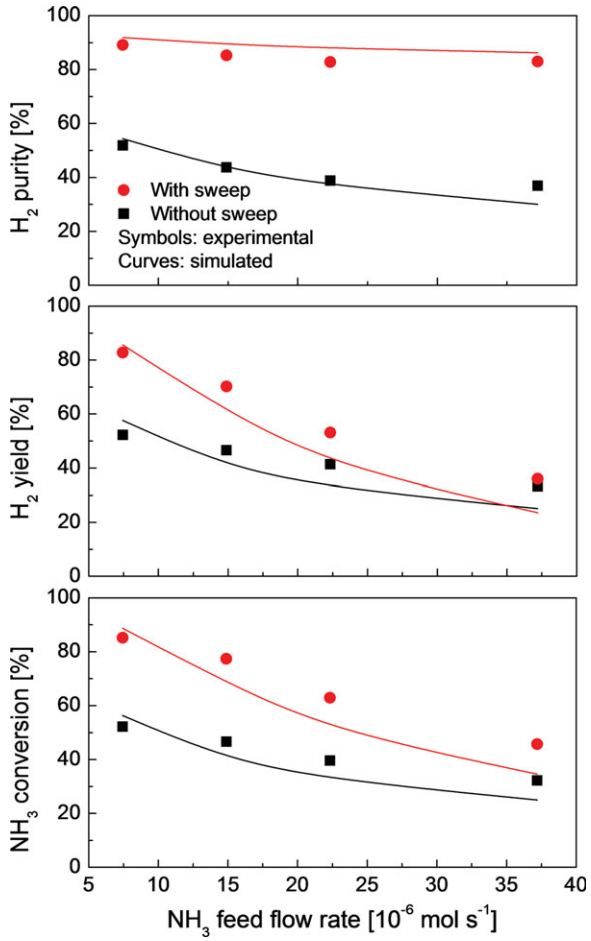

Figure 12. Effect of NH_3 feed flow rate on the performance of the BCMR-2 for NH_3 decomposition with and without sweep (T = 683 K; p_h = 100 kPa, p_l = 100 kPa; $Q_{sweep,0}$ = 7.44 × 10^{-5} mol s^{-1}; P_{H_2} = 8.1 × 10^{-7} mol m^{-2} s^{-1} Pa^{-1}, α_{H_2/NH_3} = 90, α_{H_2/N_2} = 170).

[Color figure can be viewed in the online issue, which is available at wileyonlinelibrary.com.]

rate of 7.44 × 10^{-6} mol s^{-1}. When no sweep gas was applied to the membrane reactor during the initial 30 h, no gas flow was detected on permeate side due to the lack of a driving force for gas permeation through the membrane. However, a steady H_2 flow of 5.2 × 10^{-6} mol s^{-1} was obtained in retentate stream, indicating the decomposition of NH_3 occurred on retentate side in a stable manner. The corresponding NH_3 conversion was 45%, which was much lower than the equilibrium conversion of approximate 100%. The H_2 yield and H_2 purity defined in retentate were 45 and 47%, respectively. When 7.44 × 10^{-5} mol s^{-1} sweep gas was applied to permeate side, a steady H_2 flow of 1.0 × 10^{-5} mol s^{-1} was obtained in the permeate stream, while a much smaller H_2 flow of 5.2 × 10^{-7} mol s^{-1} was detected in retentate stream. This suggests that most H_2 generated in retentate stream had permeated to the permeate side after using sweep gas. This caused a drastic increase in NH_3 conversion to 95%, with H_2 yield and purity defined in permeate as high as 90 and 94%, respectively, after the H_2 extraction. After stopping the sweep gas at 65 h, the NH_3 conversion, H_2 yield, and H_2 purity retuned to the initial values, which stayed almost the same in the additional 55 h of test time, indicating the membrane reactor was stable for as long as 120 h under the reaction conditions employed.

During the time course of NH_3 decomposition, the reaction was periodically stopped for a small interval to examine the single permeation properties of the membrane. Prior to the measurement, the experimental apparatus was flushed with N_2 and the test temperature was increased to 773 K. As shown in Figure 11, no obvious changes were observed in gas permeance during the membrane reaction, suggesting the silica membrane of the membrane reactor had good stability for gas permeation in a NH_3 atmosphere at high temperatures.

Effect of operating conditions on membrane reactor performance

Figure 12 shows the NH_3 conversion, H_2 yield and H_2 purity as a function of the NH_3 feed flow rate both with and without sweep in the BCMR-2. As the feed flow rate of NH_3 increased in the reactor, NH_3 conversion decreased both with and without sweep, due to the increased space velocity. A similar tendency was also observed in the H_2 yield with an increase in the NH_3 feed flow rate. Only a slight decrease in the H_2 purity was observed when sweep was applied, although there was a big decrease in NH_3 conversion and H_2 yield. For example, when the NH_3 feed flow rate increased from 7.44 × 10^{-6} to 3.72 × 10^{-5} mol s^{-1}, NH_3 conversion and H_2 yield decreased from 85 and 83% to 47 and 35%, respectively, while the H_2 purity only decreased from 89 to 83%. This is because the change in Da did not effectively affect the H_2 purity in the permeate stream, which was confirmed by the simulation study of membrane reactors, as shown in Figure 5. It should be noted that, after H_2 extraction with sweep, the membrane reactor performance was much superior to that without H_2 extraction in all NH_3 conversion, H_2 yield and H_2 purity. This confirmed that NH_3 decomposition for CO_x-free H_2 production was greatly enhanced by H_2 extraction using membrane reactors.

Figure 13 shows the NH_3 conversion, H_2 yield and H_2 purity as a function of reaction temperature both with and without sweep in the BCMR-2. NH_3 conversion increased with increasing reaction temperature both with and without sweep. Since the equilibrium conversion under the conditions employed was approximately 100%, the greatly increased NH_3 conversion as the reaction temperature increased could be mainly ascribed to the improved reaction rate under high temperatures, but not to the thermodynamics. However, NH_3 conversion decreased at low temperatures due to an insufficient reaction rate, which was more notable in the case without H_2 extraction. NH_3 conversion decreased much more slowly with sweep to permeate side, due to the contribution of the H_2 extraction effect on reaction performance, i.e., to achieve the same NH_3 conversion for both cases, with and without H_2 extraction, the required temperature could be lower with H_2 extraction when the other reaction conditions were identical. This suggests that the membrane reactor has the potential to reduce the reaction temperature for NH_3 decomposition, which would be very important in order to lower the energy requirement for CO_x-free H_2 production in a practical application.

Figure 14 shows the NH_3 conversion, H_2 yield and H_2 purity as a function of sweep flow rate both with and without sweep in the BCMR-2. The membrane reactor performance strongly depended on the sweep flow rate. When the sweep flow rate increased from 7.44 × 10^{-6} to 7.44 × 10^{-5} mol

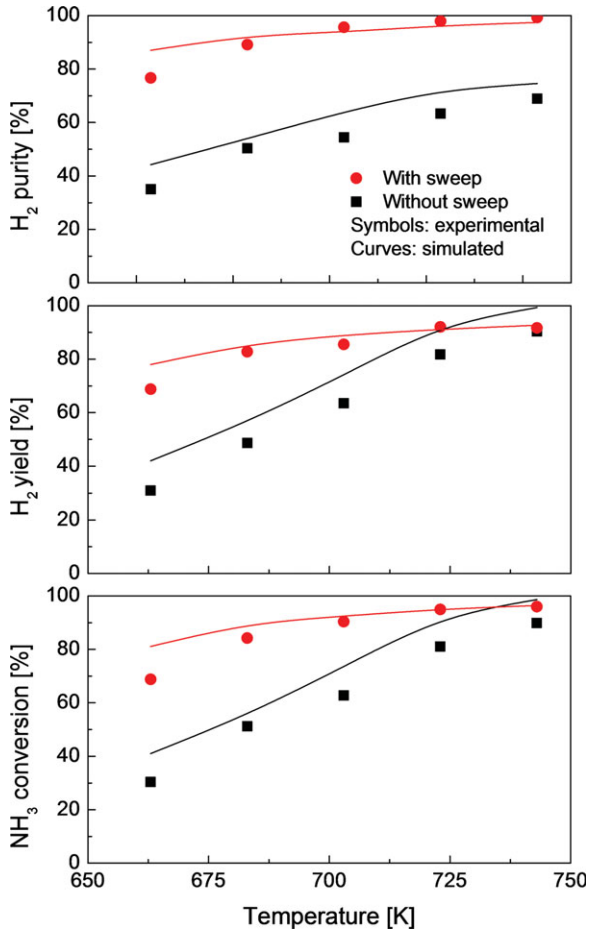

Figure 13. Effect of reaction temperature on the performance of the BCMR-2 for NH_3 decomposition with and without sweep (p_h = 100 kPa, p_l = 100 kPa; $F_{NH_3,0}$ = 7.44 × 10^{-6} mol s^{-1}, $Q_{sweep,0}$ = 7.44 × 10^{-5} mol s^{-1}; simulated curves: the effect of temperature on H_2 and N_2 permeation was considered, NH_3 permeances were assumed to be the same at 773 K).

[Color figure can be viewed in the online issue, which is available at wileyonlinelibrary.com.]

s^{-1}, the NH_3 conversion increased from 58 to 85%, the H_2 yield increased from 34 to 82%, and the H_2 purity increased from 71 to 91%. It is clear that the improvement of membrane reactor performance increased as the sweep flow rate increased. Under the given reaction conditions, membrane reactor performance is mainly determined by the amount of selective H_2 extraction removed from the reactor. H_2 permeation through the membrane is driven by the H_2 partial pressure difference between retentate and permeate streams. Therefore, a higher sweep flow rate can produce a lower H_2 partial pressure in the permeate stream, resulting in increased NH_3 conversion by increasing the driving force for H_2 permeation through the membrane.

The experimentally obtained membrane reactor performance was compared with that obtained by theoretical simulation under various operating conditions. The catalyst loading in the membrane module W_{cat}, was adopted as a single fitting parameter in the theoretical calculation, while the other parameters related to membrane characteristics (length, diameter and permeance), catalytic properties (activation energy, pre-exponential factor and exponential constant)[12] and operating conditions (temperature, pressure and flow rate) were given parameters. The value of catalyst loading in the membrane module W_{cat} was obtained by fitting experimental NH_3 conversion as a function of the NH_3 feed flow rate. As shown in Figure 12, NH_3 conversion decreased as the NH_3 feed flow rate increased due to increased space velocity, and the fitted curve was in good agreement with the experimental results with a fitted Ru catalyst amount of 4.7 × 10^{-2} g, which was in the rational loading range compared with the actual Ru catalyst weight of 3.0 × 10^{-2} g.

As shown in Figures 12–14, the simulated curves using a single fitting parameter W_{cat}, fixed at 4.7 × 10^{-2} g show a reasonable agreement with the experimental results in terms of NH_3 conversion and H_2 yield and purity with and without H_2 extraction under different operating conditions, which indicated that the proposed simulation model is applicable to the prediction of NH_3 decomposition performance in membrane reactors under various conditions. Note in Figure 13 that the simulated H_2 yield with sweep is lower than that

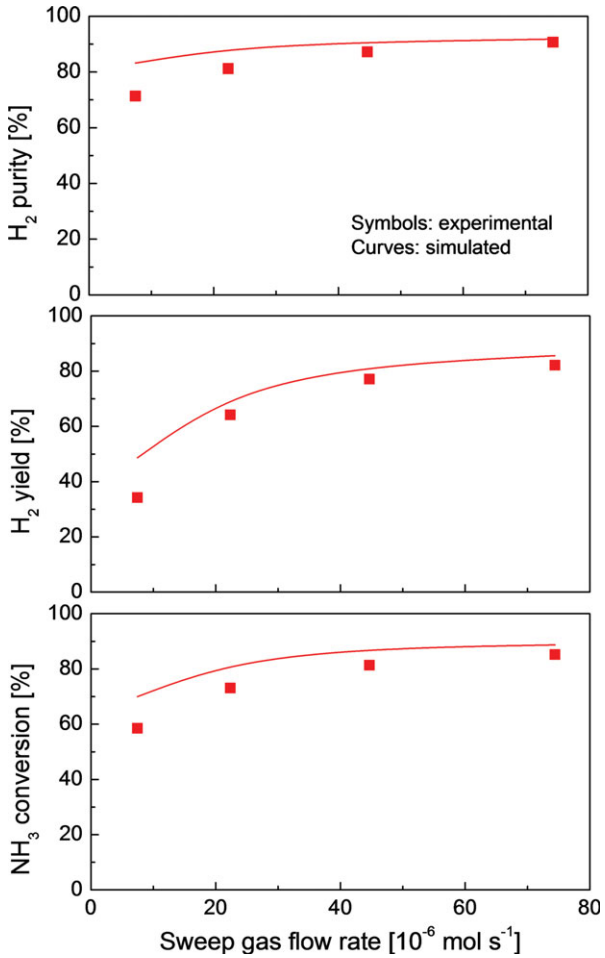

Figure 14. Effect of sweep flow rate on the performance of the BCMR-2 for NH_3 decomposition with and without sweep (T = 683 K; p_h = 100 kPa, p_l = 100 kPa; $F_{NH_3,0}$ = 7.44 × 10^{-6} mol s^{-1}; P_{H_2} = 8.1 × 10^{-7} mol m^{-2} s^{-1} Pa^{-1}, α_{H_2/NH_3} = 90, α_{H_2/N_2} = 170).

[Color figure can be viewed in the online issue, which is available at wileyonlinelibrary.com.]

without sweep above 723 K, which was mainly caused by the different definition of H_2 yield, as shown in Eq. 10 and Eq. 13. Generally, the shift of the dehydrogenation reaction in a membrane reactor after H_2 extraction could be ascribed to improved thermodynamics, such as methane steam reforming.[15,19–21,29] However, since the equilibrium conversion of NH_3 decomposition was nearly 100% under the conditions used in this study, the decomposition of NH_3 was, thus, not equilibrium-limited, and the highly enhanced NH_3 decomposition in the membrane reactor after H_2 extraction could not be attributed to improved thermodynamics. NH_3 decomposition kinetics can reportedly be expressed by the Temkin-Pyzhv model,[23] as shown in Eq. 1 used in this simulation. Compared with the forward reaction, the backward reaction, NH_3 synthesis, was too small in this study based on the thermodynamic analysis. Therefore, the Temkin-Pyzhev model could be simplified as follows

$$R = k\left(\frac{p_{NH_3}^2}{p_{H_2}^3}\right)^{\beta} \tag{15}$$

Equation 15 clearly reveals that the NH_3 decomposition rate was strongly inhibited by the presence of H_2, that is, the higher the H_2 partial pressure, the lower the NH_3 decomposition rate. This H_2 inhibition phenomenon was confirmed experimentally by several research groups under similar conditions.[11–13] Therefore, the enhanced NH_3 decomposition in the membrane reactor after H_2 extraction in this study could be mainly ascribed to the increased reaction rate, which was different from the ordinal mechanism of improved thermodynamics in most catalytic membrane reactions.

Conclusions

NH_3 decomposition in catalytic membrane reactors for CO_x-free hydrogen production was studied theoretically and experimentally. A mathematical model was formulated for a simulation study of cocurrent configuration membrane reactors with H_2-selective silica membranes showing H_2/NH_3 permeance ratios over a wide range of $10 - \infty$. Two dimensionless parameters, the Damköhler number (Da) and the permeation number (θ), were used to examine their effects, as well as that of membrane selectivity, on membrane reactor performance with respect to NH_3 conversion, H_2 yield and H_2 purity. The experimental study of pure NH_3 decomposition was conducted under temperatures of 663–743 K with NH_3 feed flow rates of 7.44×10^{-6}–7.44×10^{-5} mol s^{-1}. The effects of various operating conditions on membrane reactor performance were studied, and the results were compared with those calculated by the proposed simulation model.

(1) The simulation study of membrane reactors for NH_3 decomposition showed that the NH_3 conversion, H_2 yield and H_2 purity increased with increasing Da, and their enhancement was strongly dependent on the H_2 extraction, as well as NH_3 and N_2 permeation, through the membrane. H_2/NH_3 selectivity of 100 was high enough for a silica membrane to achieve autothermal decomposition of NH_3 with a target H_2 yield of 85% in the permeate stream, in an appropriate range of θ under the simulation conditions.

(2) The bimodal catalytic membrane reactor (BCMR) consisted of a bimodal catalytic support and H_2-selective silica membrane. Silica membranes were prepared by the sol–gel method, and showed H_2 permeances of 6.2–9.8 $\times 10^{-7}$ mol m^{-2} s^{-1} Pa^{-1} with H_2/NH_3 and H_2/N_2 permeance ratios of 110-200 and 200–700, respectively, at 773 K. The high H_2/NH_3 permeance ratios indicated that the NH_3 has an actual molecular size that is much larger than that of H_2. The temperature dependence of gas permeance suggested that the He and H_2 permeation behavior through both silica membranes was governed by the activated diffusion mechanism. The calculated activation energies for H_2 permeation were as high as 11.4 and 10.4 kJ mol^{-1} for BCMR-1 and BCMR-2, respectively, indicating that both membranes had small pore sizes.

(3) NH_3 conversion was significantly enhanced from 45 to 95% in the BCMR-1 after selective H_2 extraction at 723 K. The membrane reactor performance was stable during the test time of 120 h with respect to the catalytic activities and gas permeation properties, indicating that the membrane reactor had good stability in the NH_3 atmosphere at high temperatures.

(4) The effect of operating conditions, reaction temperature, NH_3 feed flow rate, and sweep flow rate on NH_3 conversion, H_2 yield, and H_2 purity in the BCMR-2, was investigated. The membrane reactor performance after selective H_2 extraction was very superior to that of cases studied without H_2 extraction under the same reaction conditions, which can be mainly ascribed to the improved kinetic reaction rate, rather than to thermodynamics. The experimental results were in reasonable agreement with those calculated by the proposed simulation model using catalyst weight W_{cat}, as a single fitting parameter.

Notation

Da = Damköhler number, dimensionless
E_a = activation energy, J mol^{-1}
f = dimensionless feed-side flow rate, dimensionless
F = feed-side molar flow rate, mol s^{-1}
G = purity of hydrogen, dimensionless
k = reaction rate constant, mol kg-Ru^{-1} s^{-1} $Pa^{-\beta}$
k_0 = pre-exponential factor, mol kg-Ru^{-1} s^{-1} $Pa^{-\beta}$
K_{eq} = equilibrium constant, Pa
L = membrane reactor length, m
p = partial pressure, Pa
p_h = feed-side pressure, Pa
p_l = permeate-side pressure, Pa
p_r = pressure ratio, dimensionless
P = gas permeance, mol m^{-2} s^{-1} Pa^{-1}
q = dimensionless permeate-side flow rate, dimensionless
Q = permeate-side molar flow rate, mol s^{-1}
R = reaction rate, mol kg-Ru^{-1} s^{-1}
R_g = ideal gas constant, J mol^{-1} K^{-1}
R^{max} = maximum reaction rate, mol kg-Ru^{-1} s^{-1}
R^* = dimensionless reaction rate, dimensionless
s = membrane area per unit membrane axial length, m^2 m^{-1}
T = absolute temperature, K
w_{cat} = catalyst weight per unit membrane axial length, kg-Ru m^{-1}
W_{cat} = catalyst weigh of membrane module, kg-Ru
x = feed-side mole fraction, dimensionless
X = conversion of ammonia, dimensionless
y = permeate-side mole fraction, dimensionless
Y = yield of hydrogen, dimensionless
z = axial coordinate, m

Greek letters

α = permeance ratio, dimensionless
β = exponential constant, dimensionless
θ = permeation number, dimensionless
ν = stoichiometric coefficient, dimensionless
ζ = dimensionless axial coordinate, dimensionless

Subscripts

0 = inlet of the membrane reactor
eq = equilibrium
H_2 = hydrogen
i = species i
L = outlet of the membrane reactor
N_2 = nitrogen
NH_3 = ammonia

Literature Cited

1. Schlapbach L. Hydrogen-fueled vehicles. *Nature*. 2009;460:809–811.
2. Klerke A, Christensen CH, Nørskov JK, Vegge T. Ammonia for hydrogen storage: challenge and opportunities. *J Mater Chem*. 2008;18:2304–2310.
3. Christensen CH, Johannessen T, Sørensen RZ, Nørskov JK. Towards an ammonia-mediated hydrogen economy? *Catal Today*. 2006;111: 140–144.
4. Li L, Hurley JA. Ammoni-based hydrogen source for fuel cell applications. *Int J Hydrogen Energy*. 2007;32:6–10.
5. Carlo AD, Dell'Era A, Prete ZD. 3D simulation of hydrogen production by ammonia decomposition in a catalytic membrane reactor. *Int J Hydrogen Energy*. 2011;36:11815–11824.
6. Yin SF, Xu BQ, Zhou XP, Au CT. A mini-review on ammonia decomposition catalysts for on-site generation of hydrogen for fuel cell applications. *Appl Catal A*. 2004;227:1–9.
7. Li G, Kanezashi M, Tsuru T. Highly enhanced ammonia decomposition in a bimodal catalytic membrane reactor for CO_x-free hydrogen production. *Catal Commun*. 2011;15:60–63.
8. Sørensen RZ, Nielsen LJE, Jensen S, Hansen O, Johannessen T, Quaade U, Christensen CH. Catalytic ammonia decomposition: miniaturized production of CO_x-free hydrogen for fuel cells. *Catal Commun*. 2005;6:229–232.
9. García-García FR, Ma YH, Rodríguez-Ramos I, Guerrero-Ruiz A. High purity hydrogen production by low temperature catalytic ammonia decomposition in a multifunctional membrane reactor. *Catal Commun*. 2008;9:482–486.
10. Zhang J, Xu H, Li W. High-purity CO_x-free H_2 generation from NH_3 via the ultra permeable and highly selective Pd membranes. *J Membr Sci*. 2006;227:85–93.
11. Chellappa AS, Fischer CM, Thomson WJ. Ammonia decomposition kinetics over Ni-Pt/Al_2O_3 for PEM fuel cell applications. *Appl Catal A*. 2002;227:231–240.
12. Prasad V, Karim AM, Arya A, Vlachos DG. Assessment of overall Rate expressions and multiscale, microkinetic model uniqueness via experimental data injection: Ammonia decomposition on Ru/γ-Al_2O_3 for hydrogen production. *Ind Eng Chem Res*. 2009;48:5255–5265.
13. Zheng W, Zhang J, Xu H, Li W. NH_3 decomposition kinetics on supported Ru clusters: Morphology and particle size effect. *Catal Lett*. 2007;119:311–318.
14. She Y, Han J, Ma YH. Palladium membrane reactor for the dehydrogenation of ethylbenzene to styrene. *Catal Today*. 2001;67:43–53.
15. Shu J, Grandjean PA, Kaliaguine S. Methane steam reforming in asymmetric Pd- and Pd-Ag/porous SS membrane reactors. *Appl Catal A*. 1994;119:305–325.
16. Collins JP, Way JD. Catalytic decomposition of ammonia in a membrane reactor. *J Membr Sci*. 1994;96:259–274.
17. Casanave D, Ciavarella P, Fiaty K, Dalmon J.-A. Zeolite membrane reactor for isobutene dehydrogenation: Experimental result and theoretical modeling. *Chem Eng Sci*. 1999;54:2807–2815.
18. Jeong BH, Sotowa KI, Kusakabe K. Catalytic dehydrogenation of cyclohexane in an FAU-type zeolite membrane reactor. *J Membr Sci*. 2003;224:151–158.
19. Tsuru T, Yamaguchi K, Yoshioka T, Asaeda M. Methane steam reforming by microporous catalytic membrane reactors. *AIChE J*. 2004;50:2794–2805.
20. Tsuru T, Shintani H, Yoshioka T, Asaeda M. A bimodal catalytic membrane having a hydrogen-permselective silica layer on a bimodal catalytic support: Preparation and application to steam reforming of methane. *Appl Catal A*. 2006;302:78–85.
21. Tsuru T, Morita T, Shintani H, Yoshioka T, Asaeda M. Membrane reactor performance of steam reforming of methane using hydrogen-permselective catalytic SiO_2 membranes. *J Membr Sci*. 2008;316:53–62.
22. Tsotsis TT, Champagnie AM, Vasileiadis SP, Ziaka ZD, Minet RG. The Enhancement of reaction yield through the use of high temperature membrane reactors. *Sep Sci Technol*. 1993;28:397–422.
23. Temkin MJ, Pyzhev V. Kinetics of ammonia synthesis on promoted iron catalysts. *Acta Physicochim USSR*. 1940;12:327–356.
24. Kim JH, Choi BS, Yi J. Modified simulation of methane steam reforming in Pd-membrane/packed-bed type reactor. *J Chem Eng Jpn*. 1999;32:760–769.
25. Barbieri G, Di Maio FP. Simulation of the methane steam reforming process in a catalytic Pd-membrane reactor. *Ind Eng Chem Res*. 1997;36:2121–2127.
26. Kanezashi M, Shioda T, Gunji T, Tsuru T. Gas permeation properties of silica membranes with uniform pore sizes derived from polyhedral oligomeric silsesquioxane. *AIChE J*. doi:10.1002/aic. 12716.
27. Goetsch DA, Schmit SJ. Production of hydrogen by autothermic decomposition of ammonia. Patent, US 2002/0028171 A1.
28. Hara S, Sakaki K, Itoh N. Decline in hydrogen permeation due to concentration polarization and CO hindrance in a palladium membrane reactor. *Ind Eng Chem Res*. 1999;38:4913–4918.
29. Mori N, Nakamura T, Noda K, Sakai O, Takahashi A, Ogawa N, Sakai H. Reactor configuration and concentration polarization in methane steam reforming by a membrane reactor with a highly hydrogen-permeable membrane. *Ind Eng Chem Res*. 2007;46:1952–1958.
30. Avila AM, Funke HH, Zhang Y, Falconer JL, Nobel RD. Concentration polarization in SAPO-34 membranes at high pressures. *J Membr Sci*. 2009;335:32–36.
31. Feng X, Huang RYM, Concentration polarization in pervaporation separation processes. *J Membr Sci*. 1994;92:201–208.
32. Sablani S, Goosen M, Al-Belushi R, Wilf M. Concentration polarization in ultrafiltration and reverse osmosis: a critical review. *Desalination*. 2001;141:269–289.
33. Breck DW. *Zeolite Molecular Sieves: Structure, Chemistry and Use*. New York: John Wiley & Sons, Inc; 1974:593–724.
34. van Leeuwen ME, Derivation of stockmayer potential parameters for polar fluids. *Fluid Phase Equilib*. 1994;99;1–18.
35. Kanezashi M, Yamamoto A, Yoshioka T, Tsuru T. Characteristics of ammonia permeation through porous silica membranes. *AIChE J*. 2010;56:1204–1212.
36. Kanezashi M, Yada K, Yoshioka T, Tsuru T. Organic–inorganic hybrid silica membranes with controlled silica network size: Preparation and gas permeation characteristics. *J Membr Sci*. 2010;348: 310–318.
37. de Vos RM, Verweij H. Improved performance of silica membranes for gas separation. *J Membr Sci*. 1998;143:37–51.
38. Kanezashi M, Asaeda M. Hydrogen permeation characteristics and stability of Ni-doped silica membranes in steam at high temperature. *J Membr Sci*. 2006;271:86–93.
39. Nomura M, Ono K, Gopalakrishnan S, Sugawara T, Nakao S. Preparation of a stable silica membrane by a counter diffusion chemical vapor deposition method. *J Membr Sci*. 2005;251:151–158.

Manuscript received Dec. 8, 2011, and revision received Feb. 15, 2012.